EBioMedicine 23 (2017) 136–145

Contents lists available at ScienceDirect

EBioMedicine

journal homepage: www.ebiomedicine.com

Research Paper

Salsalate Activates Skeletal Muscle Thermogenesis and Protects Mice from High-Fat Diet Induced Metabolic Dysfunction

Li Nie [a,1], Xin-Lu Yuan [a,1], Ke-Tao Jiang [b], Yu-Hui Jiang [b], Jin Yuan [a], Lan Luo [c], Shi-Wei Cui [a,*], Cheng Sun [b,*]

[a] Department of Endocrinology and Metabolic Diseases, Affiliated Hospital of Nantong University, Nantong, Jiangsu 226001, China
[b] Key Laboratory for Neuroregeneration of Jiangsu Province, Ministry of Education, Nantong University, 19 Qixiu Road, Nantong, Jiangsu 226001, China
[c] Department of Geratology, Affiliated Hospital of Nantong University, Nantong 226001, Jiangsu, China

ARTICLE INFO

Article history:
Received 18 May 2017
Received in revised form 31 July 2017
Accepted 3 August 2017
Available online 4 August 2017

Keywords:
Salsalate
Sarcolipin
Serca2
Thermogenesis
Obesity
Type 2 diabetes

ABSTRACT

Salsalate plays beneficial roles for ameliorating hyperglycemia and dyslipidemia in type 2 diabetes patients, but the underlying mechanisms are still poorly understood. In this study, by administering salsalate to mice fed with high fat diet and examining how salsalate rectifies metabolic dysfunction in these obese mice, we found that salsalate stimulated body temperature and attenuated body weight gain without affecting food intake. Our results showed that salsalate application decreased lipid accumulation in liver and epididymal white adipose tissue (eWAT), inhibited hepatic gluconeogenesis and improved insulin signaling transduction in eWAT. In addition, salsalate increased the expression of genes related to glucose and fatty acid transport and oxidation in skeletal muscle. Our results also showed that expression of genes in mitochondrial uncoupling and mitochondrial electron transport are strengthened by salsalate. Moreover, sarcolipin (Sln) and sarcoplasmic reticulum Ca^{2+} ATPase 2 (Serca2) in skeletal muscle were enhanced in salsalate-treated mice. Together, our data suggest that the beneficial metabolic effects of salsalate may depend, at least in part, on skeletal muscle thermogenesis *via* activation of mitochondrial uncoupling and the axis of Sln/Serca2a.

1. Introduction

Salicylic acid is a plant-produced hormone in response to pathogen infection (Reymond and Farmer 1998). Salsalate and aspirin are the two main pro-drugs derived from salicylic acid, which are commonly considered to be nonsteroidal anti-inflammatory drugs. The accumulating evidences suggest that these two pro-drugs of salicylic acid play beneficial efficacies against metabolic disorders in both diabetic mice and patients (Barzilay et al., 2014; Cao et al. 2011; Faghihimani et al. 2013; Kim et al. 2014; Liang et al. 2015; Smith et al. 2016; van Dam et al. 2015). Although several working models have been proposed, the underlying mechanisms still remain poorly understood. Chronic inflammation is a main causative factor for inducing obesity related insulin resistance. Therefore, the anti-inflammation action of salicylate is considered as a primary mechanism for dealing with insulin resistance (Fleischman et al. 2008; Liang et al. 2015; Pedersen and Febbraio 2010). By repressing nuclear factor IkappaB kinase subunit β, salicylate sensitizes insulin signaling to reverse hyperglycemia, hyperinsulinemia and dyslipidemia in obese rodents (Yuan et al. 2001). Moreover, it has been reported that salicylate activates AMPK *via* a direct interaction with the Ser108 residue of the β1 subunit (Hawley et al. 2012). However, salicylate still plays euglycemic effects in AMPK-β1-knockout mice fed with high fat diet, suggesting other pathways should be involved (Hawley et al. 2012; Smith et al. 2016). Most recently, one report has demonstrated that salsalate increases energy expenditure in mice by activating brown adipose tissue (BAT) (van Dam et al. 2015). Meanwhile, another study suggested that salsalate improves glucose homeostasis primarily *via* salicylate-driven mitochondrial uncoupling in brown fat tissue (BAT), skeletal muscle and liver (Smith et al. 2016). However, salsalate supplement does not alter BAT thermogenesis *in vivo* (Smith et al. 2016). Thus, skeletal muscle is likely to be the organ targeted by salsalate for thermogenesis, as liver is not a thermogenic site.

In this study, therefore, we analyzed salsalate-induced thermogenesis in skeletal muscle and the underlying molecular mechanisms. Our results showed that salsalate application attenuates body weight gain, increases body temperature and improves systemic glucose homeostasis in mice fed with HFD. Furthermore, our results revealed that salsalate

* Corresponding authors.
E-mail addresses: cuishiwei2009@163.com (S.-W. Cui), suncheng1975@ntu.edu.cn (C. Sun).
[1] These authors contributed equally to this study.

http://dx.doi.org/10.1016/j.ebiom.2017.08.004

stimulates non-shivering thermogenesis in skeletal muscle by activating mitochondrial uncoupling and the axis of Sln/sarcoplasmic reticulum Ca^{2+}-ATPase type 2a (Serca2a).

2. Materials and Methods

2.1. Animals

8 week-old male C57BL/6J mice were fed with high fat diet (HFD, 45% of calories from fat, Research Diets) or HFD with the addition of 0.5% salsalate for 40 days. Body weight and food intake were monitored every other day throughout the whole experiments. All of the animal protocols were approved by the Animal Care and Use Committee of Nantong University and the Jiangsu Province Animal Care Ethics Committee.

2.2. Glucose Tolerance Test (GTT), Insulin Tolerance Test (ITT) and Pyruvate Tolerance Test (PTT)

For GTT analysis, mice were intraperitoneally injected with D-glucose (0.5 g/kg) after an overnight fasting. For ITT analysis, mice were fasted for 6 h (from 8 am to 2 pm) and intraperitoneally injected with recombinant human insulin (0.75 IU/kg) from Eli Lilly (Indianapolis, IN). For PTT analysis, mice were fasted for 18 h and intraperitoneally injected with pyruvate (1 g/kg). Blood was taken from tail vein at 0, 15, 30, 60, 90 and 120 min after glucose or insulin or pyruvate injection and blood glucose was measured with a glucose meter from Bayer.

2.3. Analysis of In Vivo Insulin Signaling

For *in vivo* insulin signaling analysis, mice were received insulin (0.75 IU/kg) *via* intraperitoneal injection after 6 h of fasting. Five minutes after injection, gastrocnemius muscle, liver and epididymal white adipose tissue were removed and snap frozen in liquid nitrogen and stored at −80 °C until use.

2.4. Rectal Temperature Measurement

Core body temperature was measured rectally with a thermistor (Micro-Therma 2 T/ThermoWorks) during the light cycle once a week.

2.5. Biochemical Analysis

Liver ALT and AST activities were measured by commercial kits (Jiancheng, Nanjing, China) according to the manufacturer's instructions. Triglyceride, cholesterol, HDL and LDL/VLDL levels were assayed by kits (Sigma-Aldrich, USA). Plasma leptin and adiponectin concentrations were analyzed using kits from Life Technologies (Thermo Fisher Scientific). Plasma insulin was measured with an Ultra Sensitive Mouse Insulin ELISA kit from Crystal Chem (Downers Grove, IL).

2.6. RNA Extraction and Quantitative Real Time PCR (qRT-PCR)

Total RNA was extracted from cells or animal tissues using Trizol reagent (Invitrogen) and transcribed into cDNA using a synthesis kit (Bio-Rad). The gene expression analysis was performed with iQ5 Multicolor Real-Time PCR Detection System (Bio-Rad) with SYBR Green Supermix (Bio-Rad). The mRNA level was normalized to 18S as a house keeping gene. The primer sequences were listed in Supplementary Table 1.

2.7. Protein Extraction from Tissues and Cells

Cell and tissue protein extraction was described elsewhere (Sun et al. 2014). Briefly, tissues were homogenized with a bench-top homogenizer (Polytron, PT2100) in ice-cold tissue lysis buffer (25 mM Tris-HCl, pH 7.4; 100 mM NaF; 50 mM $Na_4P_2O_7$; 10 mM Na_3VO_4; 10 mM EGTA; 10 mM EDTA; 1% NP-40; 10 μg/ml Leupeptin; 10 μg/ml Aprotinin; 2 mM PMSF and 20 nM Okadaic acid). After homogenization, lysates were rotated for 1 h at 4 °C and then subjected to centrifugation at 13,200 rpm for 20 min at 4 °C. The lipid layer was removed and the supernatant was transferred into Eppendorf tubes for centrifugation. Protein concentration was quantified by using Protein Assay Kit (Bio-Rad). Equivalent protein concentration in each sample was prepared and boiled at 100 °C for 5 min in 1× Laemmli buffer. The lysates were cooled to room temperature before loading for Western blot analysis.

2.8. Western Blot Analysis

Western blot analysis was performed as previously described (Sun et al. 2014). Samples from cell lysates or tissue lysates were resolved by SDS-PAGE and then transferred to polyvinylidene fluoride (PVDF) membrane. After 1 h blocking at room temperature using 10% blocking reagent (Roche), membrane was incubated overnight with primary antibody in Tris-buffered saline solution/Tween (TBST) containing 10% blocking reagent at 4 °C. After the incubation, membrane was washed three times in TBST and incubated with secondary antibody for 1 h at room temperature. After three-time washing in TBST, membrane was developed using a chemiluminescence assay system (Roche) and exposed to Kodak exposure films. Relative protein levels were quantified by Image J program. For stripping, membrane was vigorously shaken in stripping buffer (62.5 mM Tris-HCl, pH 6.7; 2% SDS; 100 mM 2-mecaptomethanol) at 50 °C for 20 min. After stripping, membrane was washed three times in TBST.

2.9. Histology

Epididymal white adipose tissue and liver were fixed with 4% normal buffered paraformaldehyde solution and embedded in paraffin. Hematoxylin-eosin (H-E) staining was performed using standard protocols (Wang et al. 2016). Succinate dehydrogenase (SDH) activity staining was carried out on sections of gastrocnemius muscle with the method described elsewhere (Blanco et al. 1988). Skeletal muscle ultrastructural analyses were performed as described elsewhere (Gali Ramamoorthy et al. 2015). Gastrocnemius muscle samples were fixed in cacodylate buffer (0.1 M, pH 7.4) containing 2.5% glutaraldehyde and 2.5% paraformaldehyde. Post-fixation, samples were immersed in 1% osmium tetraoxide for 1 h at 4 °C, and then samples were dehydrated using graded alcohol (50, 70, 90 and 100%). Samples were oriented longitudinally and embedded in Epon 812. Ultrathin sections were cut at 70 nm and contrasted with uranyl acetate and lead citrate, and examined at 80 kv with a transmission electron microscope (JEO Ltd., Tokyo, Japan) at various magnifications by a blinded investigator. Muscle tissue from 5 mice/group was analyzed and 10 electron micrographic images were acquired for each sample to count mitochondrial numbers.

2.10. Cell Culture and Treatments

HepG2 and C2C12 cells were obtained from American Type Tissue Collection (ATCC). Cells were cultured in DMEM supplemented with 25 mM glucose, 10% fetal bovine serum (FBS) and 1% Penicillin-Streptomycin. Cells were maintained under standard conditions at 37 °C in a humidified atmosphere of 5% CO_2. To stimulate gluconeogenesis, cells were cultured in phenol-, glucose and FBS-free DMEM supplemented with 20 mM sodium lactate and 2 mM pyruvate. The starved cells were incubated with 50 μM of salsalate for 24 h. After treatment, the culture medium was collected for analyzing glucose concentration using a commercial kit (GAHK-20, Sigma-Aldrich). The cells were harvested for gene expression analysis. To analyze whether salsalate affects Serca2a expression, C2C12 cells were transfected with the plasmid expressing human SERCA2a (Plasmid #75187, Addgene) (Lytton and MacLennan 1988) using an electroporator (Nepa Gene, Japan). After transfection,

the cells were treated with 2 mM salicylate for 24 h. Total RNA and protein were extracted for measuring Serca2a expression.

2.11. Statistical Analysis

Data are presented as means ± standard error of the mean (SEM). The comparisons between two groups were performed using unpaired two-tailed Student's *t*-test. For multiple-group comparisons, one-way ANOVA with Bonferroni's *post hoc* test was applied. Significance was accepted at the level of $P < 0.05$.

3. Results

3.1. Salsalate Attenuates Body Weight Gain in Mice Fed with HFD

To recapitulate the anti-obesity effect of salsalate, mice were fed with HFD with or without salsalate for 40 days. As expected, the body weight of mice treated with salsalate was markedly decreased (Fig. 1a–b). We also monitored the food intake throughout the experiment, and the results showed that there was no significant change between vehicle- and salsalate-treated animals (Fig. 1c–d). The rectal temperature was largely up-regulated in mice treated with salsalate (Fig. 1e). To exclude the possibility that body weight decrease was due to the toxic effects of salsalate, we measured ALT and AST activities in liver, which showed that the ALT activity was decreased by salsalate, whereas the AST activity was unaltered (Fig. 1f–g). These data clearly indicate that salsalate treatment indeed prevents obesity in mice fed with HFD, which is likely due to the stimulated energy expenditure.

3.2. Salsalate Alleviates Fat Accumulation in Liver

Lipid accumulation in liver is a common consequence in mice fed with HFD, and this was confirmed by the morphology of liver (Fig. 2a). Judging by their color, livers from salsalate-treated mice are more likely to be healthy. However, salsalate unexpectedly increased the liver weight (Fig. 2b). The expression of trophic factor Vegf was enhanced, while *Hgf* was not affected (Fig. 2c). To further confirm this notion, we performed H&E staining (Fig. 2d). The results showed that lots of lipid droplets were observed in vehicle-treated mice, while few lipid droplets were occurred in salsalate-treated animals. Both the liver and plasma triglyceride levels were significantly reduced by salsalate (Fig. 2e–f). The liver cholesterol level was also decreased, while the plasma cholesterol level was unaltered (Fig. 2g–h). Furthermore, we also detected plasma lipoprotein levels and the results showed that the high density lipoprotein (HDL) was not affected

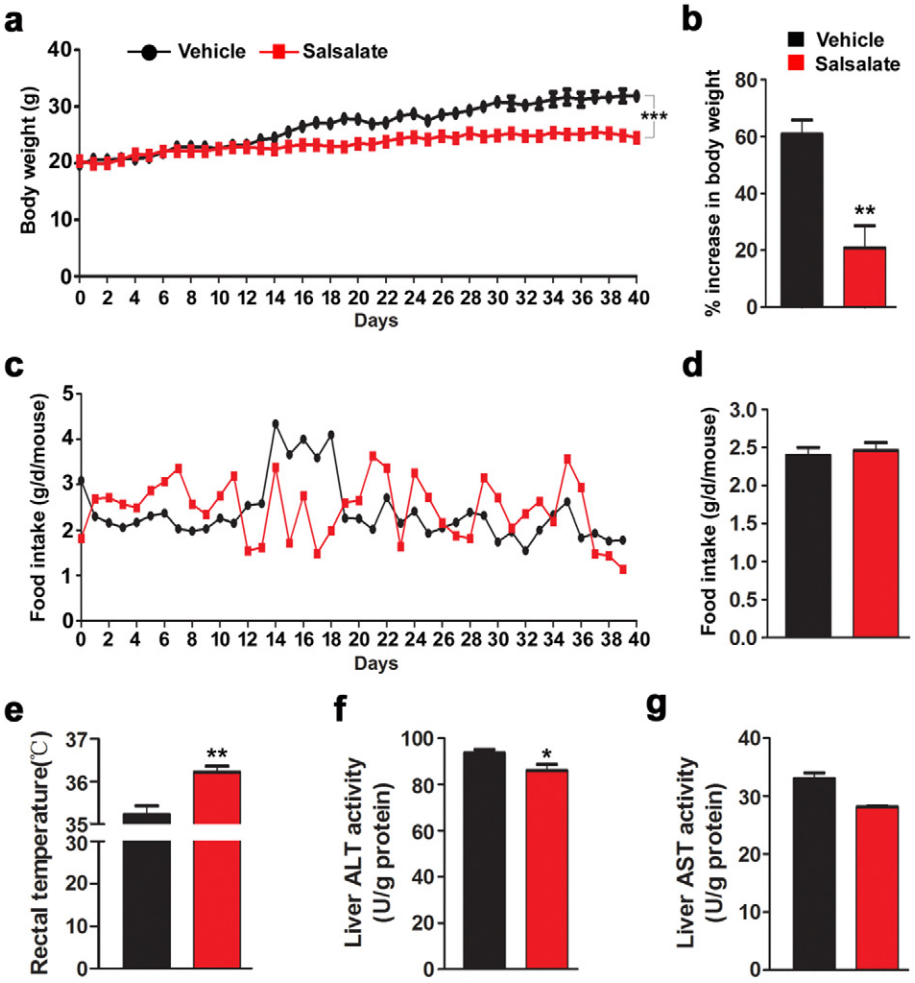

Fig. 1. Salsalate treatment attenuates body weight gain in mice fed with HFD. (a–e) The 8-week-old male mice were fed with HFD without or with salsalate for 40 days. Body weight (a–b), food intake (c–d) and body temperature (e) were monitored throughout the experiments. (f–g) The hepatic ALT (f) and AST (g) activities were measured. Data are expressed as mean ± SEM (n = 5). *$P < 0.05$ and **$P < 0.01$ by two-tailed Student's *t*-test.

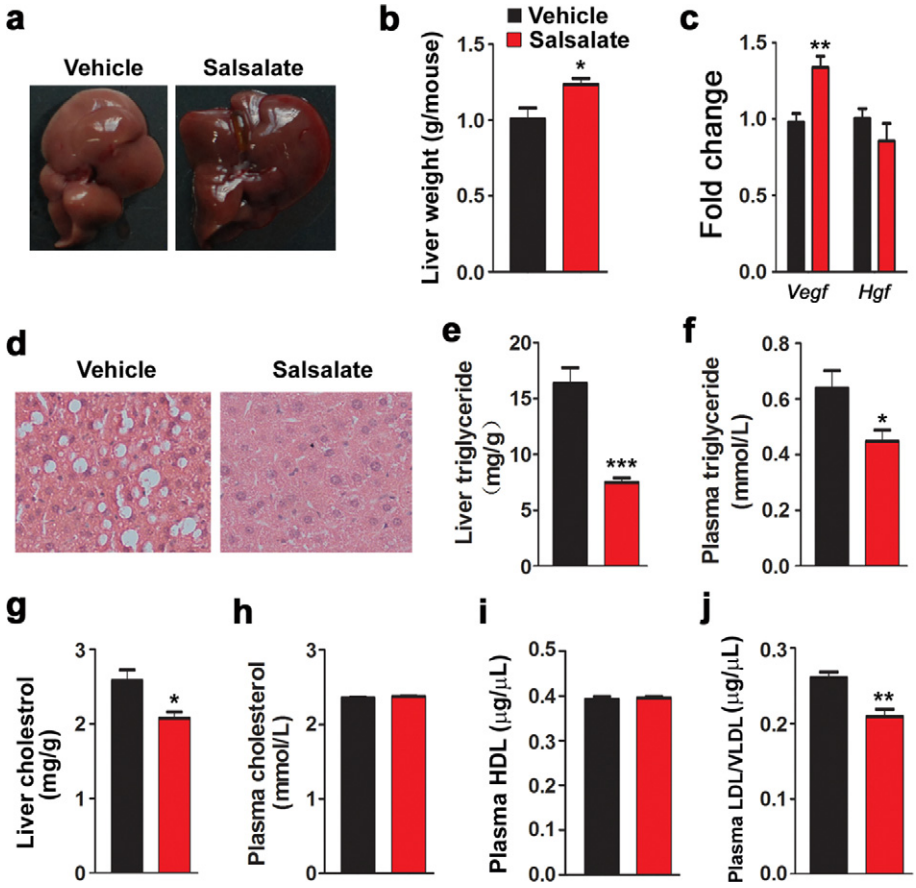

Fig. 2. Salsalate inhibits lipid synthesis in liver. (a) Liver morphology. (b) Liver weight. (c) The mRNA levels of trophic factors. (d) Liver H&E staining. (e–f) Liver triglyceride (e) and plasma triglyceride (f) were analyzed. (g–h) Liver cholesterol (g) and plasma cholesterol (h) were measured. (i–j) Plasma HDL (i) and LDL/VLDL (j) were detected. Data are expressed as mean ± SEM (n = 5). $^{*}P < 0.05$ and $^{**}P < 0.01$ by two-tailed Student's *t*-test.

by salsalate, whereas the low density lipoprotein (LDL) and very low density lipoprotein (VLDL) were both decreased (Fig. 2i–j). These data indicate that salsalate treatment attenuates lipid accumulation in liver.

3.3. Salsalate Reduces White Adipose Tissue Mass

The observed body weight loss induced by salsalate prompted us to examine whether white adipose tissue (WAT) mass was affected.

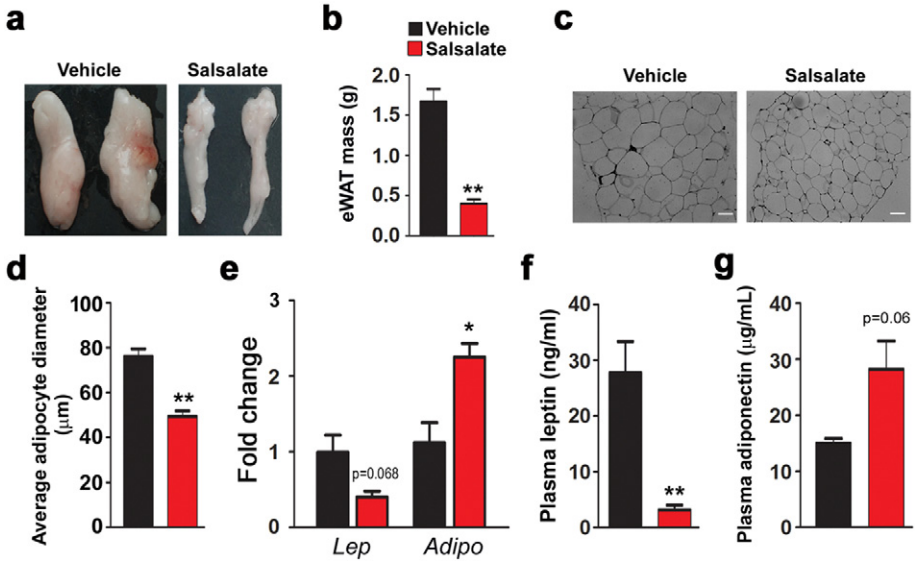

Fig. 3. Salsalate attenuates white adipose tissue biogenesis. (a) Morphology of epididymal white adipose (eWAT) tissues. (b) eWAT weight. (c) H&E staining of eWAT. (d) Average adipocyte diameter. (e) The mRNA levels of leptin and adiponectin in eWAT. (f–g) Plasma leptin (f) and adiponectin (g) were measured. Data are expressed as mean ± SEM (n = 5). $^{*}P < 0.05$ and $^{**}P < 0.01$ by two-tailed Student's *t*-test.

Indeed, the epididymal WAT (eWAT) mass was robustly reduced by salsalate (Fig. 3a). As a consequence, the eWAT weight was dramatically decreased (Fig. 3b). Furthermore, we also performed H&E staining, which showed that the cell size of adipocytes in eWAT was reduced by salsalate (Fig. 3c–d). Next, we examined the effects of salsalate on adipokine gene expression. The mRNA level of leptin in eWAT was decreased by salsalate, although the difference did not reach statistical significance. In contrast, adiponectin expression was significantly upregulated (Fig. 3e). In addition, we also measured the plasma concentrations of these two adipokines. The results showed that while the plasma leptin concentration was noticeably decreased by salsalate (Fig. 3f), the plasma concentration of adiponectin was only slightly enhanced by salsalate (Fig. 3g). The above data indicate that salsalate reduces eWAT mass and adipocyte size and regulates the gene expression of both leptin and adiponectin.

3.4. Salsalate Improves Systemic Glucose Disposal and Insulin Signaling Transduction in eWAT

Next we wanted to know whether salsalate affects systemic glucose homeostasis. To this aim, we examined the effects of salsalate on glucose metabolism and insulin signaling transduction. We performed glucose tolerance test and the data showed that salsalate increased glucose disposal as compared with vehicle-treated animals (Fig. 4a). The blood glucose level was lowered by salsalate (Fig. 4b). The plasma insulin level was slightly decreased (Fig. 4c). The insulin-stimulated glucose clearance was unaltered by salsalate from the insulin tolerance test (Fig. 4d). We next examined insulin signaling transduction in skeletal muscle, liver and eWAT. The results showed that the phospho-Akt (p-Akt) and phospho-GSK3β (p-GSK3β) in all three main insulin-responsive tissues were greatly stimulated by insulin infusion

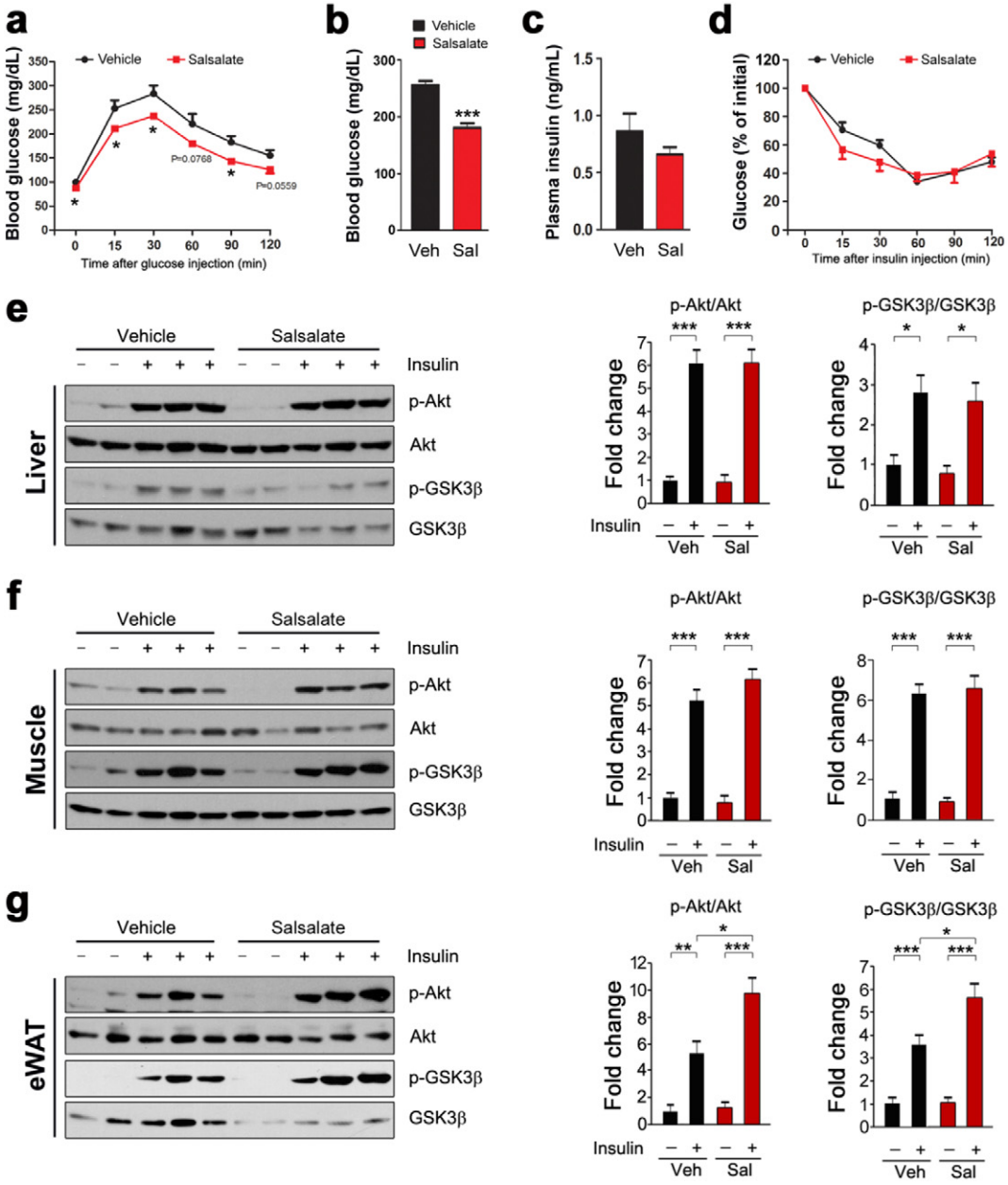

Fig. 4. Salsalate improves systemic glucose tolerance and insulin signal transduction in eWAT. (a) Glucose tolerance tests. (b) Blood glucose levels. Blood samples from mice with free access to water and food were collected by tail vein bleeding. (c) Plasma insulin concentrations. (d) Insulin tolerance tests. (e–g) The insulin signaling transduction in liver (e), skeletal muscle (f) and eWAT (g) were analyzed. Data are expressed as mean ± SEM (n = 5). $^{*}P < 0.05$, $^{**}P < 0.01$ and $^{***}P < 0.001$ by two-tailed Student's *t*-test.

(Fig. 4e–g). The salsalate treatment did not alter these stimulations in skeletal muscle and liver (Fig. 4e–f). However, the p-Akt and p-GSK3β in eWAT were further up-regulated in the presence of salsalate (Fig. 4g). Collectively, these data show that salsalate treatment improves systemic glucose disposal and stimulates insulin signaling transduction in eWAT.

3.5. Salsalate Suppresses Hepatic Gluconeogenesis

Hepatic gluconeogenesis is an important factor for regulating blood glucose level (Magnusson et al. 1992; Rizza 2010). To test whether salsalate affects hepatic gluconeogenesis, we performed pyruvate tolerance test and found that salsalate largely blocked glucose production from pyruvate (Fig. 5a). We next analyzed key transcriptional co-activator and enzymes involved in gluconeogenesis. While the expression of *G6pc* and *Pck1* were reduced by salsalate, *Ppargc1a* was unaltered (Fig. 5b). In terms of their protein levels, G6Pase and PEPCK were decreased, but PGC-1α was not altered (Fig. 5c–d). To further confirm these results, we treated HepG2 cells with salsalate and examined whether gluconeogenesis was inhibited in the cultured cells. In response to the starved condition, the gluconeogenesis was robustly up-regulated as evidenced by the increases in *G6pc* and *Pck1* expression (Fig. 5e). As expected, these stimulations were blunted in the presence of salsalate, although the change in *Pck1* was only of marginal statistical significance (Fig. 5e). For *Ppargc1a*, it was constant regardless of starvation or salsalate treatment (Fig. 5e). Moreover, we measured the glucose production released in cell culture medium and the data showed that salsalate indeed blocked glucose synthesis in starved HepG2 cells (Fig. 5f). These data clearly indicate that salsalate attenuates hepatic gluconeogenesis both *in vivo* and *in vitro*.

3.6. Salsalate Stimulates Glucose and Lipid Catabolism in Skeletal Muscle

As mentioned above, salsalate treatment leads to an increase in body temperature and thus attenuates body weight gain. We thus wanted to determine the underlying mechanisms for the increased body temperature. To do that, we analyzed the expression of genes related to heat production in BAT. The results showed that salsalate did not have noticeable effect on the expression of *Ucp1*, *Ppargc1a* and *Dio2* (Fig. 6a). Furthermore, adipogenesis-related genes, such as *Ppara* and *Pparg*, also appeared to be unaffected by salsalate (Fig. 6a). We next investigated whether inguinal WAT (iWAT) was involved in salsalate-induced heat production. As shown in Fig. 6b, adipogenesis genes *Ppara* and *Pparg* were unaltered by salsalate. *Prdm4*, *Prdm16* and *Zfp516* are commonly known as potent transcriptional factors for driving WAT browning. iWAT is a type of beige adipose tissue that could be induced into BAT-like tissue to produce heat. Our data showed that the expression of *Prdm4* and *Prdm16* were unaffected by salsalate and *Zfp516* was decreased (Fig. 6b). Genes related to heat production such as *Ucp1*, *Ppargc1a* and *Cox8b* were not altered, while *Dio2* expression was reduced (Fig. 6c).

The above data indicate that both BAT and iWAT are not the targeted tissues for salsalate-induced heat production. We thus decided to focus on thermogenesis in skeletal muscles. Gene profile results showed that the genes for fat acid transport including *Fat*, *Fabp*, *Fatp1* and *Fatp4* were significantly up-regulated by salsalate (Fig. 6d). Similar changes were also observed for fat acid hydrolysis genes (Fig. 6e). Furthermore, genes for fat acid oxidation such as *Cpt1b*, *Cpt2*, *Ppara*, *Pparg* and *Ppard* were also enhanced by the application of salsalate (Fig. 6f). In addition, we examined glucose metabolism in skeletal muscles. The genes involved in glucose transport including *Glut1* and *Glut4* were up-regulated by salsalate (Fig. 6g). Glycolysis and tricarboxylic acid cycle were also improved as evidenced by the increases in *Pfk1*, *Pk*, *Ldh*, *Sdh*, *Cs* and *Pdh* expression (Fig. 6h). The mitochondrial uncoupling and biogenesis were stimulated by salsalate, as *Ucp1*, *Ucp2* and *Ucp3* were increased (Fig. 6i). These data suggest that skeletal muscle, rather than BAT or iWAT, is the targeted tissue by salsalate for heat generation.

3.7. Salsalate Enhances Mitochondria Oxidative Capacity and SERCA2 Expression in Skeletal Muscle

The salsalate-induced increase in gene expression for glucose and fatty acid catabolism implied that mitochondrial bioenergetics was stimulated by salsalate. To test this notion, we monitored skeletal muscle mitochondrial ultrastructure by transmission electron microscopy. As shown in Fig. 7a, the mitochondrial number was not affected. The mitochondrial structure was largely destroyed as evidenced by the defects in cristae disruption and matrix density (Fig. 7b). The application of salsalate greatly prevented these defects (Fig. 7b). Next, we analyzed the expression of genes in mitochondrial electron transport chain and the results showed that all the tested genes were increased by salsalate (Fig. 7c). To further validate these results, we examined the protein levels of mitochondrial markers and found that while PHB1, SDHA and Cox IV were enhanced, VDAC and HSP60 were unaffected (Fig. 7d-e). SDH staining demonstrated that salsalate-treated mice had increased SDH activity in skeletal muscles (Fig. 7f). Since sarcoplasmic reticulum Ca^{2+} ATPase (Serca) is involved in ATP hydrolysis and heat production in skeletal muscles (Bal et al. 2012; Odermatt et al. 1998), we wanted to

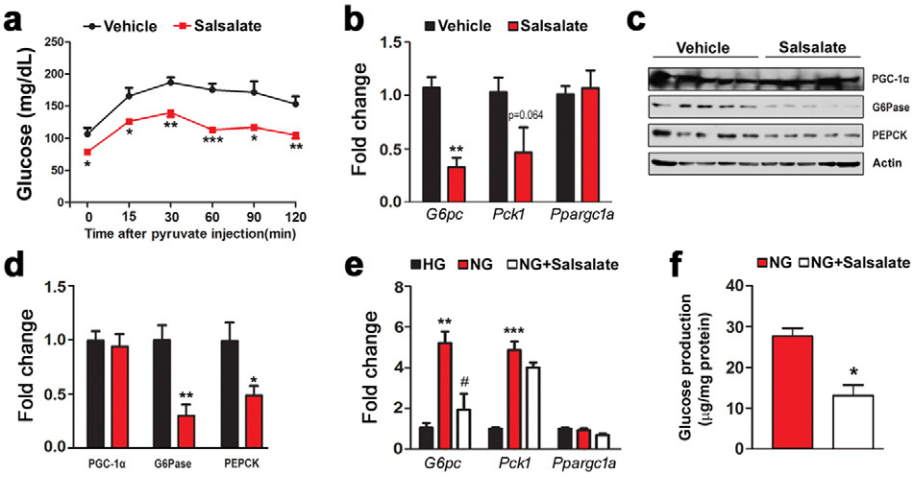

Fig. 5. Salsalate impedes hepatic gluconeogenesis. (a) Salsalate inhibits glucose production from pyruvate. (b–c) The mRNA (b) and protein (c) levels of PGC-1α, G6Pase and PEPCK. (d) Densitometric quantification of the immunoblots in (c). (e) Salsalate down-regulates gluconeogenic gene expression in the starved HepG2 cells. (f) Salsalate inhibits glucose production in the starved HepG2 cells. Data are expressed as mean ± SEM (n = 5). $^{*}P < 0.05$ and $^{**}P < 0.01$ by two-tailed Student's *t*-test.

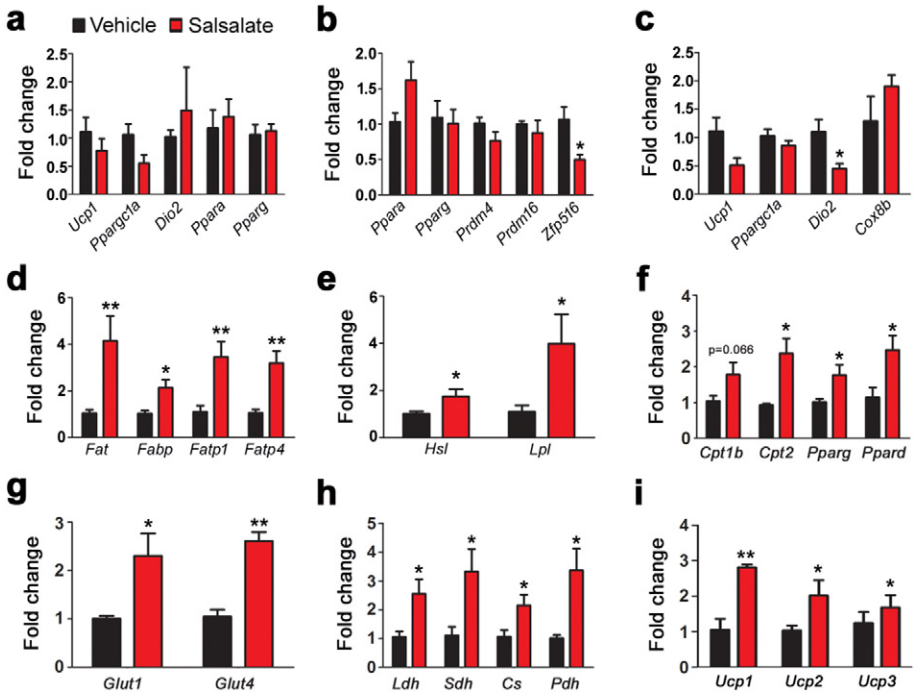

Fig. 6. Salsalate promotes glucose and lipid transport and oxidation in skeletal muscle. (a–c) The mRNA levels of genes involved in adipogenesis and heat production in BAT (a) and iWAT (b–c). (d–f) The mRNA levels of genes involved fatty acid transport (d), hydrolysis (e) and oxidation (f). (g) The expression of genes responsible for glucose transport. (h) The expression of genes in glycolysis and tricarboxylic acid cycle. (i) The expression of genes for mitochondrial uncoupling. Data are expressed as mean ± SEM (n = 5). $^{*}P < 0.05$ and $^{**}P < 0.01$ by two-tailed Student's *t*-test.

analyze whether salsalate treatment alters SERCA expression. As shown in Fig. 7g, both *Serca1a* and *Serca2a* were up-regulated by salsalate. Sln is a potent regulator of Serca in muscle for inducing uncoupling of Serca from Ca^{2+} transport and increase heat production (Bal et al. 2012; Maurya et al. 2015), it was also increased by salsalate (Fig. 7g). Western blot analysis showing that SERCA2 was markedly increased by salsalate, while SERCA1 was not affected (Fig. 7h). To further confirm these results, we transfected C2C12 cells with the plasmid expressing SERCA2a and examined whether salsalate stimulates SERCA2a expression. As expected, salsalate treatment increased SERCA2a expression in C2C12 cells (Fig. 7i), which was further confirmed by Western blot analysis (Fig. 7j). These data strongly indicate that salsalate stimulates thermogenesis in skeletal muscles by stimulating the axis of Sln/SERCA2a.

4. Discussion

Various mechanisms have been proposed to explain the beneficial effects of salsalate against obesity and type 2 diabetes. Our study suggests that salsalate treatment increases glucose and lipid transport and oxidation in skeletal muscle to generate ATP, which subsequently fuels SERCA2 to produce heat and leads to increased energy expenditure. Meanwhile, salsalate also stimulates mitochondrial uncoupling in skeletal muscle. Taken together, our data show that activation of non-shivering thermogenesis in skeletal muscle may, at least in part, be responsible for the beneficial healthy effects of salsalate.

It has been suggested that increased energy expenditure induced by salicylate-derived compounds is an efficient way for combating metabolic disorders in rats and human subjects (Hundal et al. 2002; Kim et al. 2001; Meex et al. 2011). The underlying mechanism for these bioenergetics effects are likely due to the function of salicylate to act as proton carrier (Gutknecht 1990, 1992; Smith et al. 2016). A recent study showed that salsalate application stimulates body temperature and thus attenuates body weight gain in mice fed with high fat diet by activating BAT (van Dam et al. 2015). BAT burns fatty acids and glucose to generate heat (Virtanen et al. 2009), providing a promising therapeutic target against obesity and type 2 diabetes. It has been shown that promoting BAT development is an attractive strategy for the treatment of obesity, as activated BAT dissipates energy through thermogenesis (Dempersmier et al. 2015; Oliverio et al. 2016; Qiang et al. 2012; Song et al. 2016; Tseng et al. 2008). However, our present data and previous investigation (Smith et al. 2016) showed that UCP1 in BAT was unaffected in salsalate-treated animals. Thus, additional studies are needed to examine the targeted tissue(s) for salsalate-mediated energy expenditure *in vivo*.

Clusters of UCP1-positive adipocytes with thermogenic capacity also develop in WAT in response to various stimuli such as cold exposure and hormone incubation (Ramage et al. 2016; Vitali et al. 2012; Wu et al. 2012). These adipocytes have been named beige adipocytes and tissues containing such adipocytes are known as beige adipose tissues. iWAT is a kind of beige adipose tissue, and a growing body of evidences have shown that iWAT browning is a useful strategy for dealing with obesity and its related metabolic disorders (Dodd et al. 2015; Lee et al. 2015; McDonald et al. 2015). To uncover the underlying mechanisms for salsalate-mediated energy expenditure, we have examined whether salsalate treatment leads to iWAT browning. Our data show that salsalate has no effect on BAT gene expression in iWAT, suggesting there is no iWAT browning in salsalate-treated mice. These findings indicate that enhanced energy expenditure induced by salsalate is not due to iWAT browning.

Besides BAT and beige adipose tissues, skeletal muscle is also a heat-producing organ for maintaining thermo homeostasis. Skeletal muscle accounts for ~40% of body mass and is a major consumer of metabolites (Zurlo et al. 1990). It has been suggested that skeletal muscle is an ideal organ for energy expenditure (Lowell and Spiegelman 2000; Rowland et al. 2015b). During cold exposure, skeletal muscle plays an important role for adaptive thermogenesis by expending significant amount of energy (Bal et al. 2012; Rowland et al. 2015a). Studies have also shown that skeletal muscle is a key component in diet induced thermogenesis (Astrup et al. 1989; Bombardier et al. 2013; Goto-Inoue et al. 2013). Inspired by these studies, we switched our interest from adipose tissue to skeletal muscle and aimed to uncover the underlying mechanisms for salsalate-induced thermogenesis *in vivo*. We found that salsalate

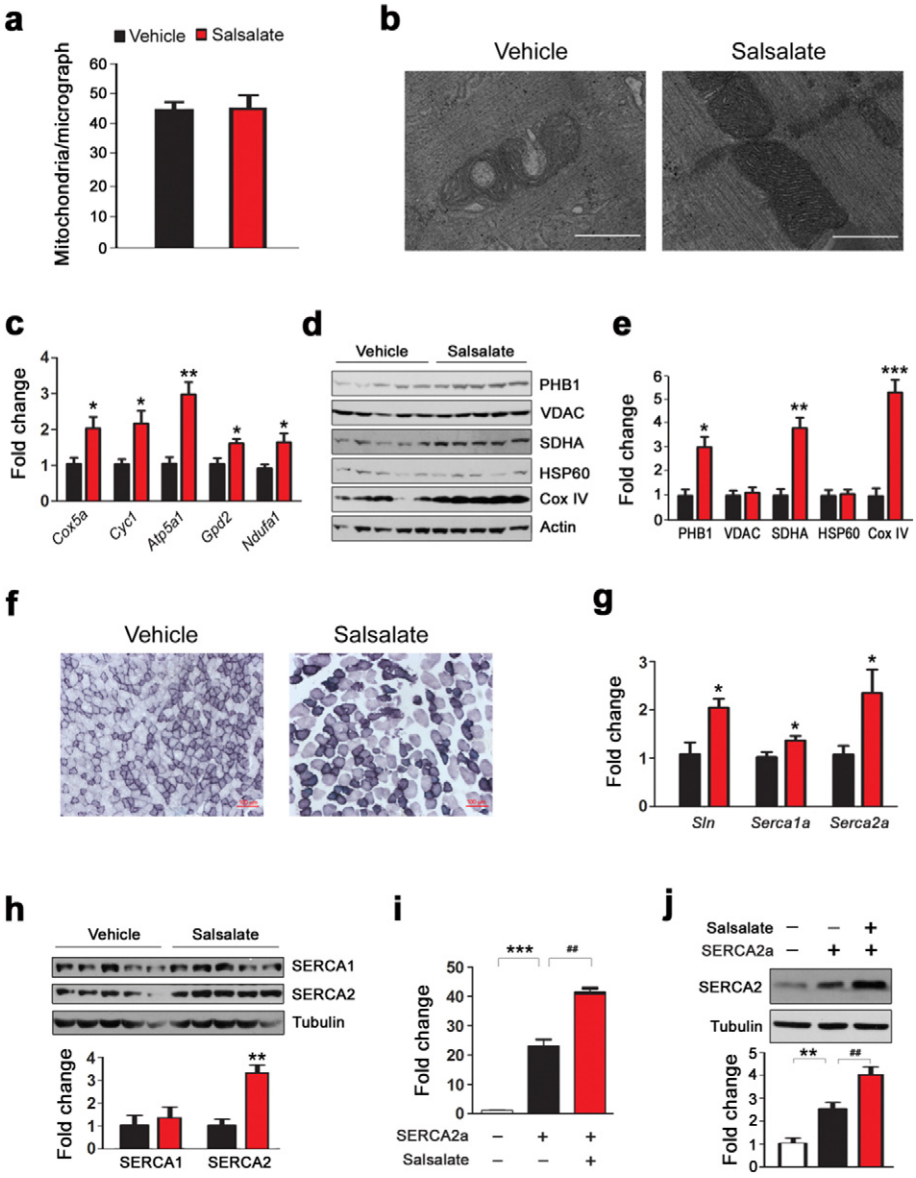

Fig. 7. Salsalate stimulates mitochondria capacity and SERCA2 expression in skeletal muscles. (a) Average mitochondrial numbers based on transmission electron micrographs at the magnification of 5 k. (n = 5). (b) Representative transmission electron micrographs at the magnification of 20 k. The scale bar represents 0.5 μm. (c) The expression of mitochondrial electron transport chain genes. (d) Western blot showing expression of different subunits of electron transport chain proteins. (e) Densitometric quantification of the immunoblots in (d). (f) Succinate dehydrogenase (SDH) staining. The scale bar represents 100 μm. (g) The expression of *Sln*, *Serca1a* and *Serca2a* in skeletal muscle. (h) Western blot showing expression of SERCA1 and SERCA2 in skeletal muscle. (i) Salicylate improves *Serca2a* expression in C2C12 cells. (j) Western blot showing the increased expression of SERCA2 by salicylate in C2C12 cells. Data are expressed as mean ± SEM (n = 5). $^{*}P < 0.05$, $^{**}P < 0.01$ and $^{***}P < 0.001$ by two-tailed Student's *t*-test. $^{\#\#}P < 0.05$ by one-way ANOVA with Bonferroni's *post hoc* test.

increases the expression of genes involved in glucose and fatty acid uptake and oxidation in skeletal muscle, suggesting that skeletal muscle is likely the target organ for salsalate-mediated thermogenesis. Indeed, mitochondrial uncoupling was stimulated by salsalate, indicating salsalate treatment switches to heat generation from ATP synthesis in mitochondria. This conclusion is in line with a recent report in which salsalate improves mitochondrial uncoupling and respiration (Smith et al. 2016).

It has been demonstrated that maintenance of Ca^{2+} ion gradient by the SERCA pump is responsible for heat production in skeletal muscle (Bal et al. 2012). Uncoupling Ca^{2+} transport and ATP hydrolysis in SERCA pump results in heat production and transient accumulation of cytosolic Ca^{2+} (Sahoo et al. 2013). In this study, we found that salsalate stimulates SERCA2 expression in skeletal muscle. Sarcolipin (Sln) - a small protein consisting 31 amino acids long - is exclusively expressed in skeletal muscle (Babu et al. 2007). Recent studies have shown that Sln is an important regulator for uncoupling Serca activity and thus plays a key role for adaptive heat generation both in cold- and diet-induced thermogenesis (Bal et al. 2012; Maurya et al. 2015). Data from the present study showed that salsalate induces an increase in Sln expression both *in vivo* and *in vitro*. Thus, we suggest that skeletal muscle is the thermogenic organ targeted by salsalate. Generation of Serca-deficient mice will further confirm this conclusion.

In addition to salsalate-mediated thermogenesis, it is also worth noting that while salsalate increases liver weight, it decreases liver triglyceride and cholesterol. We propose that salsalate might initiate liver stem cell differentiation into mature hepatocytes. Alternatively, salsalate accelerates the reprogramming other liver cells into hepatocytes. Given these predictions are true, salsalate will be beneficial for liver regeneration by inducing mature and healthy hepatocytes, which may extend the clinical application of this ancient anti-inflammatory drug. We have also found that salsalate blunts hepatic gluconeogenesis

by down-regulating G6Pase and PEPCK expression in liver, which is consistent with a previous report (Smith et al. 2016). The precise underlying mechanisms for the salsalate-mediated repression on G6Pase and PEPCK are still not clear, which will be uncovered in the future studies.

Supplementary data to this article can be found online at http://dx.doi.org/10.1016/j.ebiom.2017.08.004.

Funding Sources

This work was supported by grants from the National Natural Science Foundation of China (81471037), the Basic Research Program of Jiangsu Education Department (14KJA180006), the Six Talent Summit Project of Jiangsu Province (SWYY-051), The Scientific Program of Nantong City (MS22015126; MS22016024) and The Priority Academic Program Development (PAPD) of Jiangsu Higher Education Institutions. The funders had no role in experiment design, data collection, data analysis, interpretation and writing of the report.

Conflicts of Interest

All authors declare no conflict of interest.

Author Contributions

C.S. and S.W.C. conceived the idea. L.N., X.Y., K.J., Y.J., J.Y. L.L. and C.S. performed the experiments. C.S. designed the experiments. C.S. and L.N. analyzed the data and wrote the manuscript.

Acknowledgments

We would like to thank Dr. Weihong Qiu for his critical reading of the manuscript. We also thank Dr. Xiaoyu Liu for the technical assistance.

References

Astrup, A., Simonsen, L., Bulow, J., Madsen, J., Christensen, N.J., 1989. Epinephrine mediates facultative carbohydrate-induced thermogenesis in human skeletal muscle. Am. J. Phys. 257, E340–345.

Babu, G.J., Bhupathy, P., Carnes, C.A., Billman, G.E., Periasamy, M., 2007. Differential expression of sarcolipin protein during muscle development and cardiac pathophysiology. J. Mol. Cell. Cardiol. 43, 215–222.

Bal, N.C., Maurya, S.K., Sopariwala, D.H., Sahoo, S.K., Gupta, S.C., Shaikh, S.A., Pant, M., Rowland, L.A., Bombardier, E., Goonasekera, S.A., et al., 2012. Sarcolipin is a newly identified regulator of muscle-based thermogenesis in mammals. Nat. Med. 18, 1575–1579.

Barzilay, J.I., Jablonski, K.A., Fonseca, V., Shoelson, S.E., Goldfine, A.B., Strauch, C., Monnier, V.M., Consortium, T.-T.D.R, 2014. The impact of salsalate treatment on serum levels of advanced glycation end products in type 2 diabetes. Diabetes Care 37, 1083–1091.

Blanco, C.E., Sieck, G.C., Edgerton, V.R., 1988. Quantitative histochemical determination of succinic dehydrogenase activity in skeletal muscle fibres. Histochem. J. 20, 230–243.

Bombardier, E., Smith, I.C., Gamu, D., Fajardo, V.A., Vigna, C., Sayer, R.A., Gupta, S.C., Bal, N.C., Periasamy, M., Tupling, A.R., 2013. Sarcolipin trumps beta-adrenergic receptor signaling as the favored mechanism for muscle-based diet-induced thermogenesis. FASEB J. 27, 3871–3878.

Cao, Y., Dubois, D.C., Sun, H., Almon, R.R., Jusko, W.J., 2011. Modeling diabetes disease progression and salsalate intervention in Goto-Kakizaki rats. J. Pharmacol. Exp. Ther. 339, 896–904.

van Dam, A.D., Nahon, K.J., Kooijman, S., van den Berg, S.M., Kanhai, A.A., Kikuchi, T., Heemskerk, M.M., van Harmelen, V., Lombes, M., van den Hoek, A.M., et al., 2015. Salsalate activates brown adipose tissue in mice. Diabetes 64, 1544–1554.

Dempersmier, J., Sambeat, A., Gulyaeva, O., Paul, S.M., Hudak, C.S., Raposo, H.F., Kwan, H.Y., Kang, C., Wong, R.H., Sul, H.S., 2015. Cold-inducible Zfp516 activates UCP1 transcription to promote browning of white fat and development of brown fat. Mol. Cell 57, 235–246.

Dodd, G.T., Decherf, S., Loh, K., Simonds, S.E., Wiede, F., Balland, E., Merry, T.L., Munzberg, H., Zhang, Z.Y., Kahn, B.B., et al., 2015. Leptin and insulin act on POMC neurons to promote the browning of white fat. Cell 160, 88–104.

Faghihimani, E., Aminorroaya, A., Rezvanian, H., Adibi, P., Ismail-Beigi, F., Amini, M., 2013. Salsalate improves glycemic control in patients with newly diagnosed type 2 diabetes. Acta Diabetol. 50, 537–543.

Fleischman, A., Shoelson, S.E., Bernier, R., Goldfine, A.B., 2008. Salsalate improves glycemia and inflammatory parameters in obese young adults. Diabetes Care 31, 289–294.

Gali Ramamoorthy, T., Laverny, G., Schlagowski, A.I., Zoll, J., Messaddeq, N., Bornert, J.M., Panza, S., Ferry, A., Geny, B., Metzger, D., 2015. The transcriptional coregulator PGC-1β controls mitochondrial function and anti-oxidant defense in skeletal muscles. Nat. Commun. 6, 10210.

Goto-Inoue, N., Yamada, K., Inagaki, A., Furuichi, Y., Ogino, S., Manabe, Y., Setou, M., Fujii, N.L., 2013. Lipidomics analysis revealed the phospholipid compositional changes in muscle by chronic exercise and high-fat diet. Sci Rep 3, 3267.

Gutknecht, J., 1990. Salicylates and proton transport through lipid bilayer membranes: a model for salicylate-induced uncoupling ans swelling in mitochondria. J. Membr. Biol. 115, 253–260.

Gutknecht, J., 1992. Aspirin, acetaminophen and proton transport through phospholipid bilayers and mitochondrial membranes. Mol. Cell. Biochem. 114, 3–8.

Hawley, S.A., Fullerton, M.D., Ross, F.A., Schertzer, J.D., Chevtzoff, C., Walker, K.J., Peggie, M.W., Zibrova, D., Green, K.A., Mustard, K.J., et al., 2012. The ancient drug salicylate directly activates AMP-activated protein kinase. Science 336, 918–922.

Hundal, R.S., Petersen, K.F., Mayerson, A.B., Randhawa, P.S., Inzucchi, S., Shoelson, S.E., Shulman, G.I., 2002. Mechanism by which high-dose aspirin improves glucose metabolism in type 2 diabetes. J. Clin. Invest. 109, 1321–1326.

Kim, J.K., Kim, Y.J., Fillmore, J.J., Chen, Y., Moore, I., Lee, J., Yuan, M., Li, Z.W., Karin, M., Perret, P., et al., 2001. Prevention of fat-induced insulin resistance by salicylate. J. Clin. Invest. 108, 437–446.

Kim, S.H., Liu, A., Ariel, D., Abbasi, F., Lamendola, C., Grove, K., Tomasso, V., Ochoa, H., Reaven, G., 2014. Effect of salsalate on insulin action, secretion, and clearance in nondiabetic, insulin-resistant individuals: a randomized, placebo-controlled study. Diabetes Care 37, 1944–1950.

Lee, M.W., Odegaard, J.I., Mukundan, L., Qiu, Y., Molofsky, A.B., Nussbaum, J.C., Yun, K., Locksley, R.M., Chawla, A., 2015. Activated type 2 innate lymphoid cells regulate beige fat biogenesis. Cell 160, 74–87.

Liang, W., Verschuren, L., Mulder, P., van der Hoorn, J.W., Verheij, J., van Dam, A.D., Boon, M.R., Princen, H.M., Havekes, L.M., Kleemann, R., et al., 2015. Salsalate attenuates diet induced non-alcoholic steatohepatitis in mice by decreasing lipogenic and inflammatory processes. Br. J. Pharmacol. 172, 5293–5305.

Lowell, B.B., Spiegelman, B.M., 2000. Towards a molecular understanding of adaptive thermogenesis. Nature 404, 652–660.

Lytton, J., MacLennan, D.H., 1988. Molecular cloning of cDNAs from human kidney coding for two alternatively spliced products of the cardiac Ca2+−ATPase gene. J. Biol. Chem. 263, 15024–15031.

Magnusson, I., Rothman, D.L., Katz, L.D., Shulman, R.G., Shulman, G.I., 1992. Increased rate of gluconeogenesis in type II diabetes mellitus. A 13C nuclear magnetic resonance study. J. Clin. Invest. 90, 1323–1327.

Maurya, S.K., Bal, N.C., Sopariwala, D.H., Pant, M., Rowland, L.A., Shaikh, S.A., Periasamy, M., 2015. Sarcolipin is a key determinant of the basal metabolic rate, and its overexpression enhances energy expenditure and resistance against diet-induced obesity. J. Biol. Chem. 290, 10840–10849.

McDonald, M.E., Li, C., Bian, H., Smith, B.D., Layne, M.D., Farmer, S.R., 2015. Myocardin-related transcription factor A regulates conversion of progenitors to beige adipocytes. Cell 160, 105–118.

Meex, R.C., Phielix, E., Moonen-Kornips, E., Schrauwen, P., Hesselink, M.K., 2011. Stimulation of human whole-body energy expenditure by salsalate is fueled by higher lipid oxidation under fasting conditions and by higher oxidative glucose disposal under insulin-stimulated conditions. J. Clin. Endocrinol. Metab. 96, 1415–1423.

Odermatt, A., Becker, S., Khanna, V.K., Kurzydlowski, K., Leisner, E., Pette, D., MacLennan, D.H., 1998. Sarcolipin regulates the activity of SERCA1, the fast-twitch skeletal muscle sarcoplasmic reticulum Ca2+−ATPase. J. Biol. Chem. 273, 12360–12369.

Oliverio, M., Schmidt, E., Mauer, J., Baitzel, C., Hansmeier, N., Khani, S., Konieczka, S., Pradas-Juni, M., Brodesser, S., Van, T.M., et al., 2016. Dicer1-miR-328-Bace1 signalling controls brown adipose tissue differentiation and function. Nat. Cell Biol. 18, 328–336.

Pedersen, B.K., Febbraio, M.A., 2010. Diabetes: treatment of diabetes mellitus: new tricks by an old player. Nat. Rev. Endocrinol. 6, 482–483.

Qiang, L., Wang, L., Kon, N., Zhao, W., Lee, S., Zhang, Y., Rosenbaum, M., Zhao, Y., Gu, W., Farmer, S.R., et al., 2012. Brown remodeling of white adipose tissue by SirT1-dependent deacetylation of Ppargamma. Cell 150, 620–632.

Ramage, L.E., Akyol, M., Fletcher, A.M., Forsythe, J., Nixon, M., Carter, R.N., van Beek, E.J., Morton, N.M., Walker, B.R., Stimson, R.H., 2016. Glucocorticoids acutely increase Brown adipose tissue activity in humans, revealing species-specific differences in UCP-1 regulation. Cell Metab. 24, 130–141.

Reymond, P., Farmer, E.E., 1998. Jasmonate and salicylate as global signals for defense gene expression. Curr. Opin. Plant Biol. 1, 404–411.

Rizza, R.A., 2010. Pathogenesis of fasting and postprandial hyperglycemia in type 2 diabetes: implications for therapy. Diabetes 59, 2697–2707.

Rowland, L.A., Bal, N.C., Kozak, L.P., Periasamy, M., 2015a. Uncoupling protein 1 and sarcolipin are required to maintain optimal thermogenesis, and loss of both systems compromises survival of mice under cold stress. J. Biol. Chem. 290, 12282–12289.

Rowland, L.A., Bal, N.C., Periasamy, M., 2015b. The role of skeletal-muscle-based thermogenic mechanisms in vertebrate endothermy. Biol. Rev. Camb. Philos. Soc. 90, 1279–1297.

Sahoo, S.K., Shaikh, S.A., Sopariwala, D.H., Bal, N.C., Periasamy, M., 2013. Sarcolipin protein interaction with sarco(endo)plasmic reticulum Ca2+ ATPase (SERCA) is distinct from phospholamban protein, and only sarcolipin can promote uncoupling of the SERCA pump. J. Biol. Chem. 288, 6881–6889.

Smith, B.K., Ford, R.J., Desjardins, E.M., Green, A.E., Hughes, M.C., Houde, V.P., Day, E.A., Marcinko, K., Crane, J.D., Mottillo, E.P., et al., 2016. Salsalate (salicylate) uncouples mitochondria, improves glucose homeostasis, and reduces liver lipids independent of AMPK-beta1. Diabetes 65, 3352–3361.

Song, N.J., Choi, S., Rajbhandari, P., Chang, S.H., Kim, S., Vergnes, L., Kwon, S.M., Yoon, J.H., Lee, S., Ku, J.M., et al., 2016. Prdm4 induction by the small molecule butein promotes white adipose tissue browning. Nat. Chem. Biol. 12, 479–481.

Sun, C., Wang, M., Liu, X., Luo, L., Li, K., Zhang, S., Wang, Y., Yang, Y., Ding, F., Gu, X., 2014. PCAF improves glucose homeostasis by suppressing the gluconeogenic activity of PGC-1alpha. Cell Rep. 9, 2250–2262.

Tseng, Y.H., Kokkotou, E., Schulz, T.J., Huang, T.L., Winnay, J.N., Taniguchi, C.M., Tran, T.T., Suzuki, R., Espinoza, D.O., Yamamoto, Y., et al., 2008. New role of bone morphogenetic protein 7 in brown adipogenesis and energy expenditure. Nature 454, 1000–1004.

Virtanen, K.A., Lidell, M.E., Orava, J., Heglind, M., Westergren, R., Niemi, T., Taittonen, M., Laine, J., Savisto, N.J., Enerback, S., et al., 2009. Functional brown adipose tissue in healthy adults. New Engl. J. Med. 360, 1518–1525.

Vitali, A., Murano, I., Zingaretti, M.C., Frontini, A., Ricquier, D., Cinti, S., 2012. The adipose organ of obesity-prone C57BL/6J mice is composed of mixed white and brown adipocytes. J. Lipid Res. 53, 619–629.

Wang, M., Luo, L., Yao, L., Wang, C., Jiang, K., Liu, X., Xu, M., Shen, N., Guo, S., Sun, C., et al., 2016. Salidroside improves glucose homeostasis in obese mice by repressing inflammation in white adipose tissues and improving leptin sensitivity in hypothalamus. Sci Rep 6, 25399.

Wu, J., Bostrom, P., Sparks, L.M., Ye, L., Choi, J.H., Giang, A.H., Khandekar, M., Virtanen, K.A., Nuutila, P., Schaart, G., et al., 2012. Beige adipocytes are a distinct type of thermogenic fat cell in mouse and human. Cell 150, 366–376.

Yuan, M., Konstantopoulos, N., Lee, J., Hansen, L., Li, Z.W., Karin, M., Shoelson, S.E., 2001. Reversal of obesity- and diet-induced insulin resistance with salicylates or targeted disruption of Ikkbeta. Science 293, 1673–1677.

Zurlo, F., Larson, K., Bogardus, C., Ravussin, E., 1990. Skeletal muscle metabolism is a major determinant of resting energy expenditure. J. Clin. Invest. 86, 1423–1427.